

RESEARCH

Open Access



Potential role of susceptibility-weighted imaging in the diagnosis of non-neoplastic pediatric neurological diseases

Ahmed S. Abdelrahman^{*} , Yasser A. Abbas, Sarah M. Abdelwahab and Nivan Hany Khater

Abstract

Background: This study aimed to assess the added value and current applications of SWI in the diagnosis of pediatric non-neoplastic neurological diseases, including its ability to characterize hemorrhage in various brain lesions and its important role in the evaluation of both arterial as well as venous ischemic brain lesions.

Results: Forty pediatric patients with a median age of 9 years were included in our prospective study; 23 were males and 17 females. SWI had a significantly higher detection rate than conventional MRI for traumatic brain injury (TBI) lesions, hemorrhagic lesions in acute necrotizing encephalopathy (ANEC), and cavernoma lesions ($p = 0.005$, $p = 0.038$, and $p = 0.046$, respectively). The sensitivity, specificity and accuracy of SWI for the detection of venous ischemic insult was 88.9%, 50%, and 76.9% respectively. SWI was significantly better than the conventional MRI ($p = 0.046$) for the detection of chronic ischemic brain insults and ischemic lesions with added hemorrhagic components.

Conclusion: SWI is a technique with reasonable acquisition time that could improve the diagnostic performance of MRI for the evaluation of various pediatric non-neoplastic neurological diseases.

Keywords: Pediatric, Non-neoplastic, Neurological diseases, SWI, MRI

Background

Susceptibility-weighted imaging (SWI) is an impressive magnetic resonance imaging (MRI) technique highly susceptible for the detection of blood products, iron deposition and calcifications [1]. Because of its distinctive capability to detect differences in tissue susceptibility, it can narrow the differential diagnosis of many neurologic disorders.

SWI is generated from a gradient-echo MRI sequence and is thus of high spatial resolution that can accentuate the magnetic properties of deoxygenated blood, ferritin, calcium and hemosiderin [2]. SWI has shown its significance in the diagnostic work-up of different ischemic lesions, vascular malformations, traumatic brain injury

(TBI), neurodegenerative disorders and cerebral tumors [3]. SWI is acquired in 3D mode, allowing thinner slices and smaller voxel sizes to be obtained. Parallel imaging is used to shorten imaging time by reconstructing magnitude and phase data, displaying them independently, and then processing them to form a clinically effective phase mask [4].

The SWI technique is a non-invasive tool that can provide us with crucial data about the brain perfusion and venous drainage of the ischemic areas [5]. SWI strongly accentuates the paramagnetic properties of venous deoxygenated blood and extravascular blood products, and thus it is a very useful imaging modality for studying the cerebral veins in both acute and chronic pediatric brain ischemia [5]. It is a powerful complementary sequence to diffusion-weighted images (DWI) in detecting hemorrhage within the infarct as well as thrombosis within the vessels [6].

*Correspondence: dr_ahmedsamy@yahoo.com
Radiology Department, Faculty of Medicine, Ain Shams University, Cairo, Egypt

Moyamoya disease (MMD) is a relatively uncommon cerebrovascular disease that is characterized by progressive stenosis of the distal end of both internal carotid arteries with resultant formation of a network of collateral circulation, named moyamoya vessels [7]. Increased conspicuity of the deep medullary veins (DMVs) on SWI makes it an important tool for staging the grade and severity of MMD.

Advanced magnetic resonance (MR) imaging techniques, particularly SWI, have been proven to play an important role in determining the severity of traumatic brain injury (TBI) and, as a result, in the management and rehabilitation of affected patients [8]. Traumatic brain injury is an important entity characterized by varying degrees of cognitive and functional impairment in the pediatric age group [9]. SWI permits more accurate localization and even better identification of punctate and small intraparenchymal hemorrhages, even in some cases it is better than computed tomography (CT) for the detection of subarachnoid and intraventricular hemorrhage [9].

Acute necrotizing encephalopathy (ANEC) is an uncommon but distinct kind of encephalopathy that affects people all over the world [10]. ANEC is an uncommon consequence of influenza and other viral infections that has been linked to intracranial cytokine storms, resulting in blood–brain barrier disruption but without direct viral invasion or parainfectious demyelination [11]. It is a progressive and devastating disease, and the presence of hemorrhage is associated with a poor prognosis, with SWI being the most sensitive MR technique for detecting petechial hemorrhage [11].

Last but not least, SWI can aid in the identification of low flow vascular malformations and is regarded as one of the most effective techniques for diagnosing occult low flow vascular malformations [12]. Occult vascular malformations include capillary telangiectasia, developmental venous anomalies, and cerebral cavernous malformations [13].

The aim of this study was to evaluate the potential role of SWI in the evaluation of paediatric non-neoplastic neurological diseases, its capability to characterise haemorrhagic brain lesions and its crucial role in the diagnosis of both arterial and venous ischemic brain lesions.

Methods

Patients

Our prospective study was performed in our institutional hospital from January 2020 till December 2020. Forty children with neurological manifestations referred from the pediatric department to the radio-diagnosis department have participated in this study. A clear proper history was taken from the clinician as

well as guardians of all the patients (e.g., onset of the presenting neurological symptom, duration, and course of the symptom, past history of similar symptoms, history of neurological or non-neurological diseases, previous medication, the available laboratory data and chronic diseases as diabetes mellitus.). The MRI study was done for all the pediatric patients after taking written consent from the parents or responsible family according to the rules of our ethical committee. The inclusion criteria included pediatric patients with neurological manifestations as post-traumatic head injury, lateralization symptoms and disturbed conscious level. Exclusion criteria were patients with neoplastic lesions, patients` above 18 years of age and patients with contraindications to MRI as cochlear implants and metallic implants.

Technique of examination

MRI study was performed using a 1.5 T machine (Philips Ingenia) using a dedicated head coil, study time was around 15 min. The patient lies supine, headfirst, and asked to breathe quietly if old enough. Sedative medications with vital data monitoring were used for some patients in this study.

A routine non-contrast MRI examination was done for all the patients which included T1WI, T2WI and FLAIR sequences. FOV 256 × 200 mm, average slice thickness: 4 mm, average interval 4 mm. T1WI: (TR: 120, TE: 21), T2WI: (TR: 5288, TE: 120), FLAIR: (TR: 1100/2800, TE: 130).

An additional DWI and ADC map were added (TR: 3580, TE: 112). Time of flight (TOF) magnetic resonance angiography (MRA) and venography (MRV) sequences (TR: 17, TE: 6.9) were also taken according to the clinical manifestations, especially those with a suspected ischemic pathology.

High-resolution SWI sequences were performed with a TR, 24 ms; TE, 34 ms and a flip angle of 10. Four sets of images were generated in the SWI sequence dataset. An original magnitude image and a filtered phase or phase mask were initially obtained. The original magnitude and phase data were multiplied by each other to produce a combined SWI processed magnitude image. Finally, a minimum intensity projection (minIP) image was used to display the combined processed magnitude data using contiguous sections of thickness from 8 to 16 mm in the axial plane. In children, a typical minIP thickness of 16 mm with 8 contiguous 2 mm slices was obtained. In neonates, however, to avoid misinterpretation of localization or partial volume, a smaller field of view and a minIP thickness of 8 mm was used with 8 contiguous 1 mm slices.

Table 1 Clinical, imaging features and the final diagnosis of all lesions

Presenting clinical symptoms	Final diagnosis	Imaging data	Potential SWI addition
Ten children with history of trauma with altered consciousness level	10 patients with TBI	5 patients with DAI 2 patients with subdural hemorrhage 2 patients with hemorrhagic brain contusion 1 patient with DAI, hemorrhagic brain contusion and intraventricular hemorrhage 3 patients with hemorrhagic ANEC 2 patients with ANEC	SWI revealed a greater number of DAI lesions than the conventional MRI
Five children with fever followed by deterioration of conscious level after an attack of respiratory/gastrointestinal infection	5 patients with ANEC		SWI detect a greater number of hemorrhagic lesions than conventional MRI SWI also detect hemorrhagic lesions that was not seen by the conventional MRI imaging in one patient
Five children with headache, focal neurological deficits, or seizures	5 patients with cavernoma	3 patients with cavernoma detected by conventional MRI 2 patients with cavernoma confirmed by SWI and serial follow up imaging	SWI detect a greater number of hemorrhagic areas within cavernoma lesions than conventional MRI SWI discovered two cavernoma that was not visible in the conventional MRI imaging
Thirteen children with vomiting, headache, focal neurological deficit, seizures or coma	9 patients with venous ischemic brain lesion	6 patients with venous sinus thrombosis 3 patients with cortical vein thrombosis The follow up imaging and clinical data revealed absent venous sinus or cortical vein thrombosis in 4 patients (hypoglycemia was found in 2 patients, brain abscess was also found in 2 patients)	SWI diagnosed 8 patients (6 with venous sinus thrombosis and 2 with cortical vein thrombosis) and missed one case of cortical vein thrombosis)
Seven children with neurological deficit	7 patients with ischemic brain insult	4 patients with moyamoya 3 patients with infarction	SWI revealed additional microhemorrhage in 1 case of moyamoya SWI revealed additional microhemorrhage in 2 patients with infarction SWI equivocally diagnosed 1 patient with infarction and prominent draining vein

Analysis of data

Imaging analysis

MRI studies were independently analyzed by two radiologists with 7 and 5 years of experience in neuropediatric imaging and if the result was discordant, a final result was taken by a consensus. Both radiologists were blinded to the results of the conventional MRI.

The number of the hemorrhagic non-ischemic brain lesions in SWI was counted and later on, compared to the number of hemorrhagic lesions detected by the conventional imaging. The SWI diagnosis of arterial ischemia, as well as the venous sinus and cortical vein thrombosis, were compared to the final standard reference that considered both the imaging and the clinical information; the imaging data was based upon MRI with DWI, non-contrast MRA, non-contrast MRV, and CT, whereas the clinical data included serial clinical follow-up. The confidence of arterial ischemic brain lesion diagnosis by the SWI and the conventional MRI studies was assessed and graded as confidently diagnostic study, fairly diagnostic study, and equivocal study.

Statistical analysis

Recorded data were analyzed using Statistical Package for Social Science (IBM Corp, released 2013. IBM SPSS statistics for windows, V. 22.0. Armonk, NY, USA). Parametric quantitative data were expressed as mean \pm standard deviation (SD). Non-parametric data were expressed as median with inter-quartile range (IQR). Qualitative data were described as frequency and percentage.

The non-parametric Wilcoxon signed ranks test was used to compare the detection rate of the hemorrhagic brain lesions between the conventional and SWI MRI sequences. The Pearson Chi-Square test was used for comparing the binary categorical variable related to the venous ischemic brain lesion. The non-parametric Wilcoxon Rank Sum test was performed to compare the variable related arterial ischemic insult. The interobserver agreement was determined using cross-tabulation and Cohen's kappa coefficient (K), and Kappa agreement was interpreted as slight agreement (0.01–0.20), fair agreement (0.21–0.40), moderate agreement (0.41–0.60), substantial agreement (0.61–0.80) and almost perfect agreement (0.81–1). *P*-value < 0.05 was considered significant as the confidence interval and the accepted margin of error was set to 95% and 5% respectively.

Results

Forty children with different non-neoplastic neurological insults were examined, 23 (57.5%) were boys and 17 (42.5%) were girls with a median patient's age of 9 years (IQR = 6 years and 6 months, the patient age range was one year and 6 months to 18 years). Table 1 demonstrates the clinical, imaging features and the final diagnosis of all lesions.

Hemorrhagic non-ischemic brain lesions were seen in 20 patients and the most noted pathology in the current study was TBI (10 patients presented with diffuse axonal injury (DAI), subdural hemorrhage, intraventricular hemorrhage, or hemorrhagic brain contusions), followed by acute necrotizing encephalopathy (5 patients) and cavernomas (5 patients in whom two cavernomas were only evident in the SWI sequence).

Several hemorrhagic lesions were seen in many patients, and the number of all hemorrhagic lesions detected by SWI was 62 lesions (41 hemorrhagic lesions in TBI, 11 in ANEC and 10 in cavernomas), yet the number of all hemorrhagic lesions detected by the conventional MRI were 26 lesions (16 in TBI, 4 in ANEC and 6 in cavernomas) (Figs. 1, 2, 3). The detection rate of SWI for all hemorrhagic brain lesions, TBI lesions, hemorrhagic lesions in ANEC and cavernoma lesions was significantly higher than that of conventional MRI technique ($p < 0.001$, $p = 0.005$, $p = 0.038$ and $p = 0.046$ respectively) (Table 2).

SWI diagnosed ten patients with venous ischemic insults (8 true positive and 2 false positive) manifested as an intravenous thrombus within the venous sinus (6 patients) and cortical vein thrombosis (4 patients; two were true positive and two were false positive) (Fig. 4). The sensitivity of SWI sequence as compared to the standard reference was 88.9% with specificity, PPV, NPV and accuracy of 50%, 80%, 66.7%, and 76.9% respectively (Table 3).

The SWI was of significantly greater value than the conventional MRI for the detection of chronic ischemic brain insult and ischemic lesions with added hemorrhagic component ($p = 0.046$). SWI confidently diagnosed four patients with ischemic brain disease; three were moyamoya (Fig. 5) and one case was microhemorrhages in infarction. The SWI fairly diagnosed two patients; one was moyamoya disease with added hemorrhagic component and one was an infarction with microhemorrhage. An infarction with prominent draining veins was equivocally diagnosed by the SWI (Table 4).

(See figure on next page.)

Fig. 1 A six-year-old child with a history of trauma. **A, B** Axial T2 WI and T1 WI at level of lateral ventricles show an area of altered signal in the right forceps minor and subtle area in the left corona radiata. **C, D** Axial T2 WI and T1 WI at a higher-level show subtle area of high T2 WI signal in the right centrum semiovale with no matched abnormality in the T1WI. **E, F** SWI MinIP sequences show multiple hemorrhagic foci/microbleeds in both frontal white matter and right occipital regions (black arrow). Picture of DAI

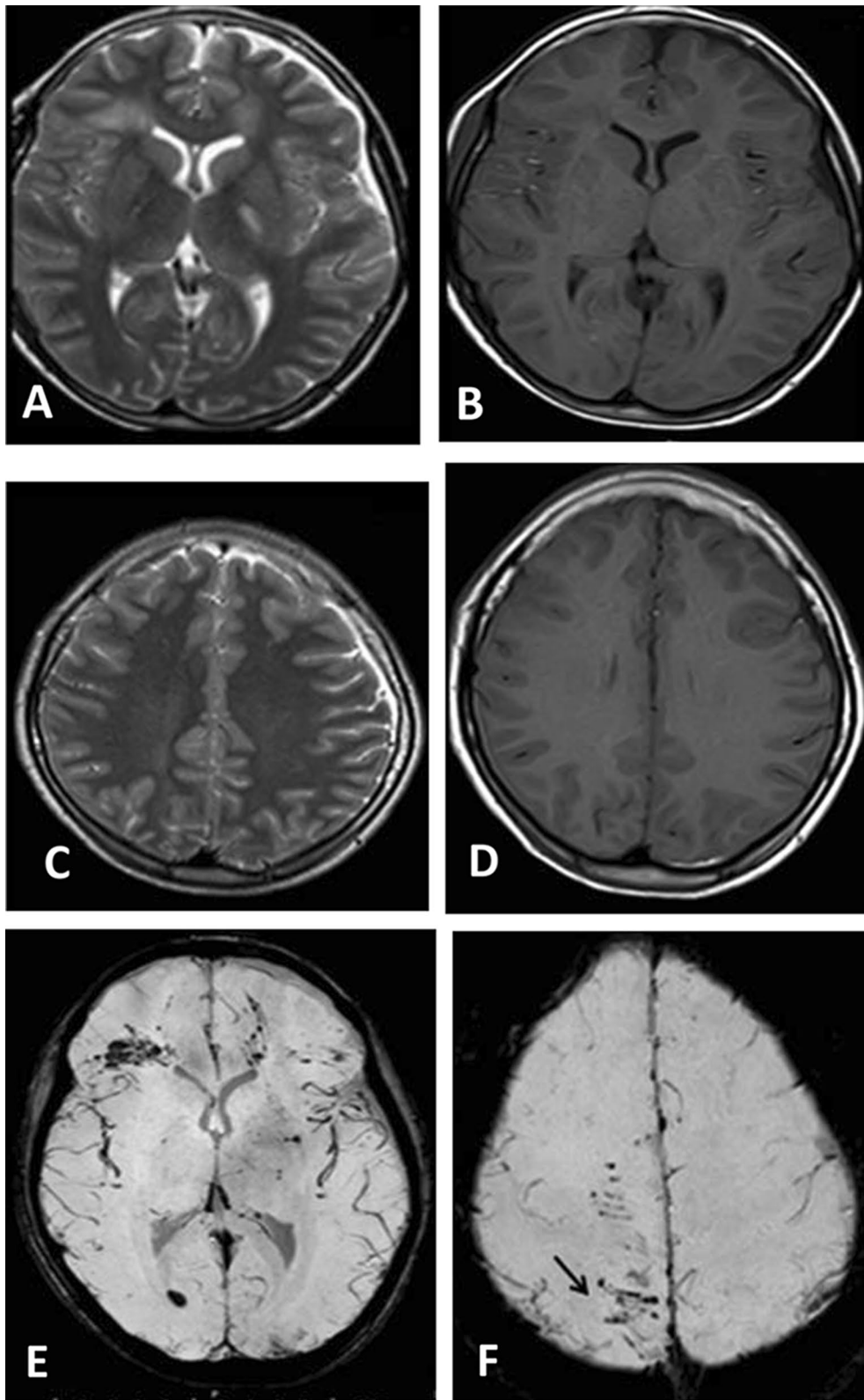


Fig. 1 (See legend on previous page.)

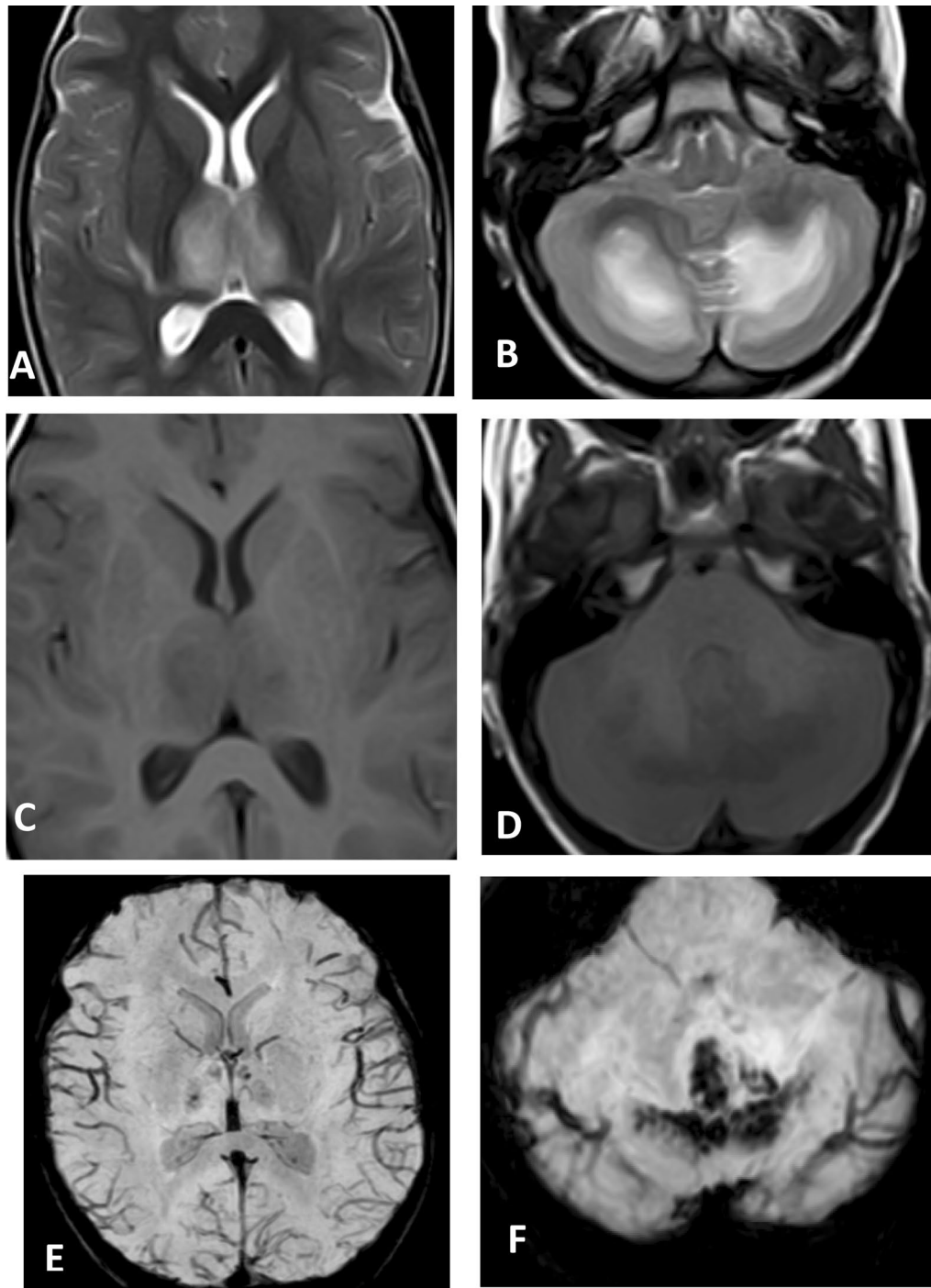


Fig. 2 A male child presented with acute necrotizing encephalopathy of childhood. **A, B** Axial T2 images showing the classical trilaminar bilateral symmetrical appearance in both thalami and both cerebellar hemispheres. **C, D** Axial T1 images show lesions of low signal. **E, F** SWI sequences show hemorrhagic component with subtle hemorrhage in thalami and huge hemorrhagic component in the posterior fossa

The matched cases between both observers for hemorrhagic brain lesions, venous ischemic lesions, arterial ischemic lesions, and all lesions were 18/20 (90%), 12/13

(92.3%), 6/7(85.7%) and 36/40 (90%) respectively. An almost perfect inter-observer agreement was noted for hemorrhagic brain lesions ($k=0.865$, $p<0.001$), venous

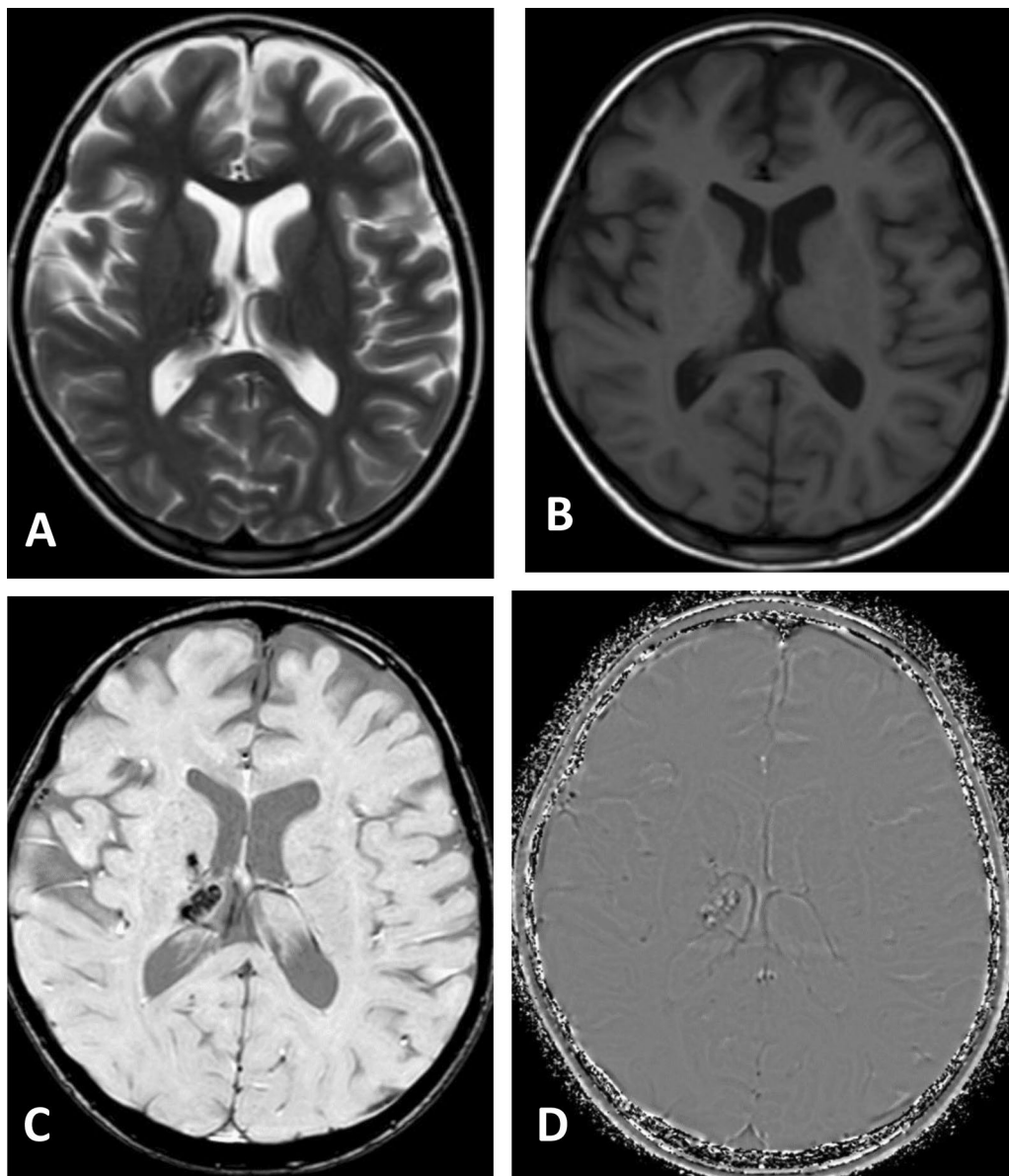


Fig. 3 A female child with accidentally discovered cavernoma. **A, B** Axial T2 WI shows a suspicious area of abnormal signal in the right thalamus region on T2 WI (**A**) inconspicuous on T1 (**B**). **C, D** SWI (**C**) clearly demonstrates the cavernoma and SWI filtered phase images (**D**) shows lesion hyperintense similar to the vessels

Table 2 Number of hemorrhagic brain lesions in the SWI and conventional MRI

Hemorrhagic lesions	SWI	Conventional MRI	Z score	P-value	Sig
TBI	41	16	-2.84	0.005	S ⁺
ANEC	11	4	-2.07	0.038	S ⁺
Cavernoma	10	6	-2	0.046	S ⁺
All lesions	62	26	-3.874	<0.001	S ⁺

⁺ Significant

ischemic lesions ($k=0.806$, $p=0.003$) and all lesions ($k=0.875$, $p<0.001$), yet a substantial agreement was noted for arterial ischemic lesions ($k=0.731$, $p=0.006$) (Table 5).

Discussion

SWI is a superb protocol of increasing use, now being included in MRI protocols of a number of neurological diseases because of its high sensitivity. Any tissue that has a different susceptibility than its surrounding structures such

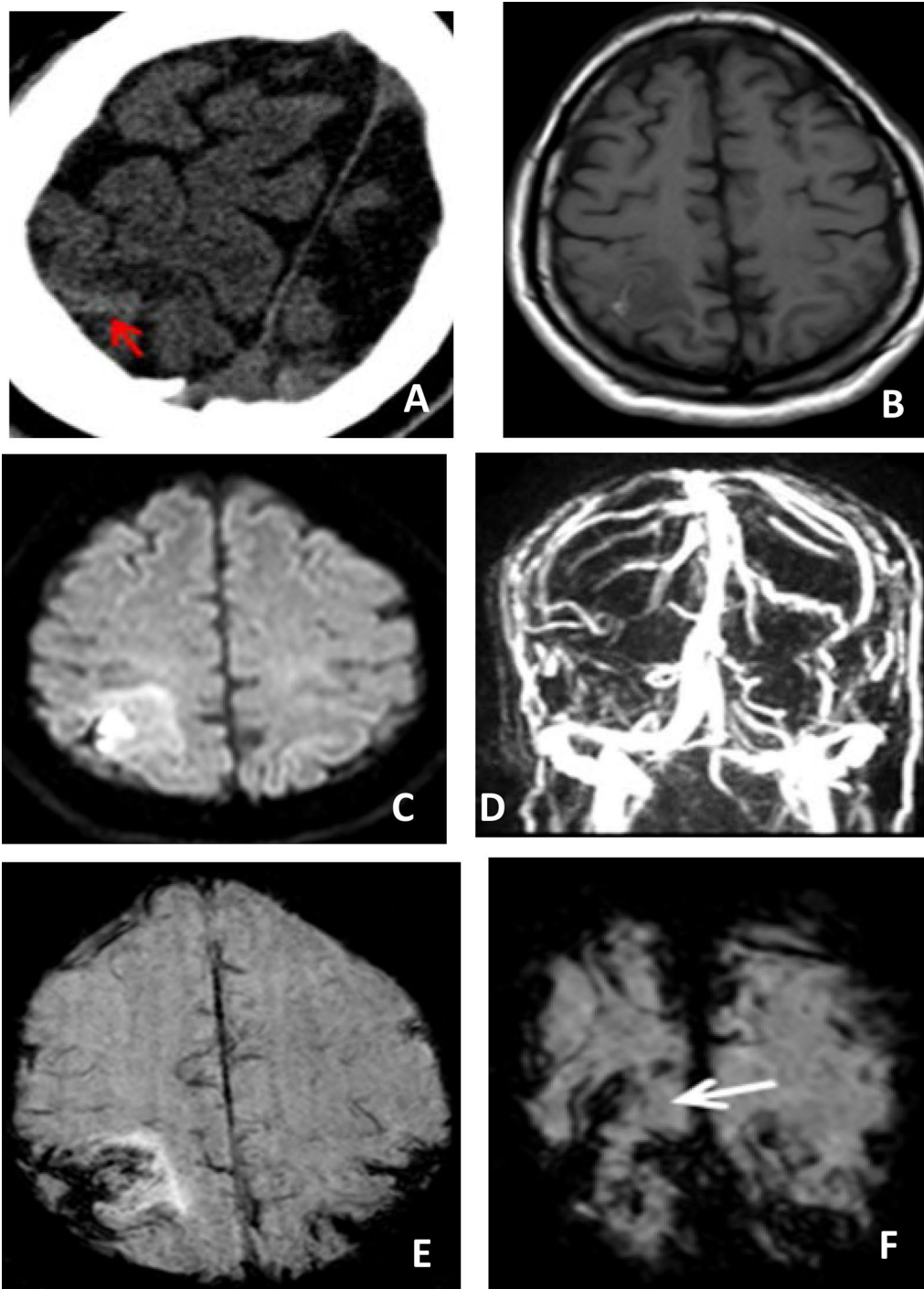


Fig. 4 A male children presented with neurological manifestations, CT was done at first, then one day later with a worsening patient symptom, MRI was done, and it revealed venous infarction secondary to cortical vein thrombosis. **A** CT study axial cut performed one day before MRI revealed a subtle undiagnosed right-sided hyperdense cortical vein (red arrow). **B** MRI study was done the following day with worsening patient symptoms and T1 WI (**B**) showed a right high frontal lesion of low signal with faint hyperintense signal within. **C** DWI showed restricted diffusion. **D** MRV study was normal. **E, F** SWI showed a hemorrhagic venous infarction (**E**) with prominent thrombosed cortical veins higher up (white arrow) (**F**)

Table 3 The diagnostic performance of SWI for detection of venous ischemic brain lesion

TP	TN	FP	FN	Sensitivity	Specificity	PPV	NPP	Accuracy
8	2	2	1	88.9%	50%	80%	66.7%	76.9%

TP true positive, TN true negative, FP false positive, FN false negative

as deoxygenated blood, hemosiderin, ferritin and calcium can be easily detected by SWI [14].

SWI was previously known as blood oxygen level-dependent imaging (BOLD) as it provides us with information on the blood oxygen level in vessels especially the venous drainage and its signal intensity. The uncoupling of oxygen supply and demand in hypoperfused brain tissue may result in a relative rise of deoxyhemoglobin levels and a decrease of oxyhemoglobin levels in tissue capillaries and draining veins, which accounts for the greater visibility of veins in this region [5]. SWI allows early detection of hemorrhage, identifies microbleeds and can detect an intravascular clot in the acute stage. It has also been found to provide information on tissue viability focusing on the signal intensity within the draining veins to evaluate ischemic penumbra [7].

In the current study, SWI revealed one case with a hypointense signal and slightly prominent veins draining the infarct area and extending beyond the infarct, suggestive of penumbra. Sorimachi et al. [15] demonstrated that dilated cortical veins detected on SWI may represent regions with higher oxygen extraction fractions due to chronic ischemia.

Four cases of moyamoya disease were demonstrated on SWI, of which one showed an added hemorrhagic component. According to Horie et al. [16], SWI can be used to assess the severity of moyamoya disease by analyzing the number of draining intramedullary veins, giving the brush-like appearance or “brush-sign”. The number of the conspicuous deep medullary veins draining into the subependymal veins was classified: stage 1, mild (<5); stage 2, moderate (5–10); and stage 3, severe (10) [16]. In our study, two patients were stage 2 and two were classified as stage 3.

Our study revealed nine children with cerebral venous thrombosis, 6/9 was venous sinus thrombosis which was correctly diagnosed by the SWI, while 3/9 were cortical vein thrombosis, where the SWI missed one case of them which was subtle in the SWI and interpreted as normal cortical vein (FN), yet the follow-up CT and MRI done two and 4 days later respectively proved that it was cortical vein thrombosis, in the other hand, the SWI overestimated prominent cortical veins as cortical vein thrombosis in two children (FP). SWI can detect the venous infarcts which are frequently hemorrhagic, even the small microbleeds and is a good technique to demonstrate the thrombosed veins [17]. Our study agreed with Thomas et al. [18] who

found that susceptibility-weighted imaging facilitates the detection of venous sinus thrombosis otherwise difficult to detect in conventional MRI images.

An emergency cerebrovascular disease that requires urgent diagnosis to minimize potential complications is TBI. We had 10 cases of TBI, most of which were diffuse axonal injury appearing as scattered microbleeds which were inconspicuous on the T1 WI yet more evident on the SWI with an excellent demonstration by the filter phase as regards signal, size and number of microbleeds with a p-value of 0.005. Our results were similar to those of Sinha et al. [19] and Sultan et al. [20], who found that the SWI was superior to conventional MRI for microbleed detection, with p-values of 0.001 and 0.006, respectively. Hamdeh et al. [21] and Babikian et al. [22] both emphasized the sensitivity and significant role of SWI in detecting the size, distribution, and number of hemorrhagic lesions in DAI. According to Ashwal et al. [23], SWI may provide more accurate prognostic information regarding the long-term neurophysiologic outcome as regards TBI. Lawrence et al. [24] study revealed that using SWI to detect DAI microbleed gives an objective early marker of damage severity following trauma.

Acute necrotizing encephalopathy of children is a fulminant form of encephalopathy resulting in rapid and progressive symptoms of brain dysfunction [25]. The classic picture is concentric laminar lesions in both thalami [26]. However, the presence of hemorrhage is a sign of severity and its demonstration is crucial to assess the outcome. This study included only 5 patients with ANEC because it is a rare entity, of which SWI was able to show the hemorrhagic component very clearly with small petechial hemorrhages seen not only in the thalami but also in the cerebellum and brain stem. SWI was an excellent modality and was the only sequence capable of adding more detail as regards the small petechiae of hemorrhage. This is in agreement with Manara et al. [27] who emphasized that the SWI is a crucial study for demonstrating tiny petechial hemorrhage, which is frequently obscured in the conventional MRI sequences.

Five cases of cavernomas were included in our study, two presented with headache, one with seizure, one with arm numbness and one with leg weakness. All cavernomas were clearly evident and excellently demonstrated on SWI sequence especially on the filter phase, while two of them were obviously seen in the SWI and overlooked on the conventional sequences due to their small size. Sultan et al.

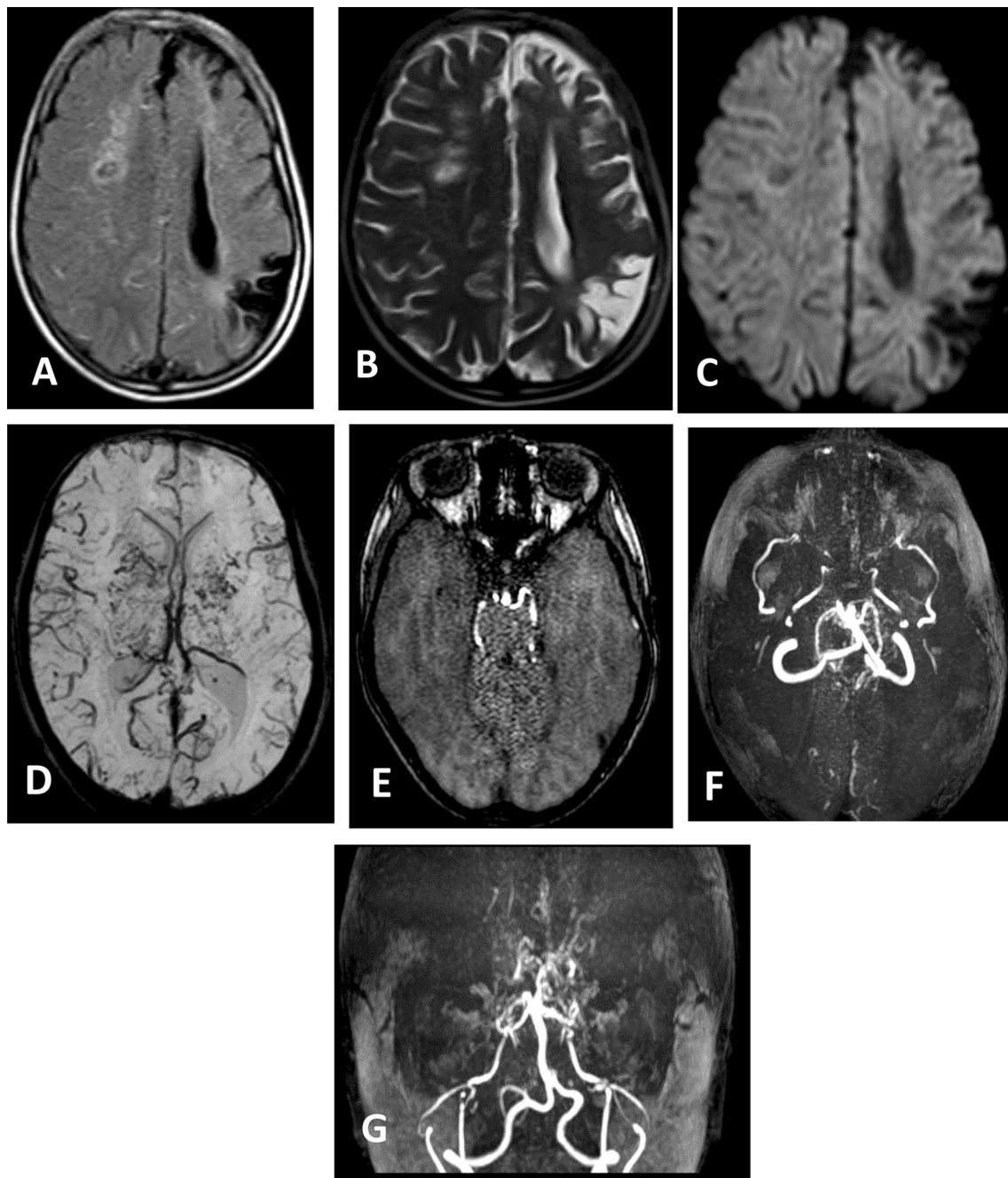


Fig. 5 A nine years old male presented with right-sided weakness and diagnosed with moyamoya disease. **A, B** Axial FLAIR (**A**) and T2 WI (**B**) show left frontal and parietal area of encephalomalacia due to repeated ischemia with right corona radiate ischemic foci and lacunar infarcts. **C** Axial DWI No recent infarcts were seen. **D** SWI shows classic brush sign of deep medullary veins at the basal ganglia and thalamus draining into the subependymal vein (stage 3). **E, F, G** Source image (**E**) and post-processing MRA (**F, G**) show attenuated both middle cerebral arteries, anterior cerebral arteries and distal part of ICA

[20] also observed a greater SWI detection rate for cavernoma, with a p -value of 0.004. Our study agreed with Sparcia et al. [28] who stated that SWI is the best MRI sequence for cavernoma detection.

The high spatial resolution of SWI and increased contrast of SWI increased the confidence of the radiologists in the diagnosis, especially for the less experienced ones. The SWI demonstrated a substantial to almost complete

Table 4 Comparison between SWI and conventional MRI for arterial ischemia diagnosis

Ischemic stroke	SWI	Conventional MRI	Z-test	p-value
Confidently diagnostic study	4	1	- 2.000	0.046 ⁺
Fairly diagnostic study	2	4		
Equivocal study	1	2		

⁺ Significant

Table 5 Inter-observer agreement of the SWI regarding hemorrhagic lesion, venous ischemic lesion, arterial ischemic lesion, and all lesions

	Matched case	K	95% CI	P-value
Hemorrhagic lesion	18 (90%)	0.865	0.690–1	< 0.001*
Venous ischemic lesion	12 (92.3%)	0.806	0.447–1	0.003*
Arterial ischemic lesion	6 (85.7%)	0.731	0.252–1	0.006*
All lesions	36 (90%)	0.875	0.759–0.991	< 0.001*

* Significant P-value

interobserver agreement for identification of hemorrhagic, ischemic, and the whole lesions, which was consistent with El-Serougy et al. [29] study, which revealed an almost perfect agreement for the detection of cerebral microbleed with a k value of 0.84. Potential problems connected to the use of SWI, according to Bosemani et al. [30], include pitfalls owing to variations in blood oxygenation levels, blood flow, potential pitfalls related to magnetic field intensity, pitfalls due to misinterpretation of localization on minIP images, and mimickers such as gas. It's critical to be aware of these pitfalls to avoid misinterpretation or misdiagnosis.

Limitation

Our study had limitations, the first was the relatively small number of patients. Our results were also obtained on a 1.5 T MRI which may not directly translate to imaging at 3 T, as the field strength is known to affect sensitivity for detection of hemorrhage and vessels. Lastly, we recommend the use of quantitative susceptibility mapping; a novel sequence under several trials in the staging of hemorrhage and in observing iron content changes over time.

Conclusion

SWI is an important imaging sequence with a potential role and with various clinical applications in the diagnosis of a group of important pediatric neurological diseases. A number of diseases can dramatically benefit from this imaging sequence in both diagnosis, management and follow-up.

Abbreviations

SWI: Susceptibility-weighted imaging; MRI: Magnetic resonance imaging; TBI: Traumatic brain injury; DWI: Diffusion-weighted imaging; MMD: Moyamoya disease; MR: Magnetic resonance; CT: Computed tomography; ANEC: Acute necrotizing encephalopathy; MRA: Magnetic resonance angiography; MRV: Magnetic resonance venography; minIP: Minimum intensity projection; DAL: Diffuse axonal injury; DMVs: Deep medullary veins; BOLD: Blood oxygen level-dependent imaging; TP: True positive; TN: True negative; FP: False positive; FN: False negative.

Acknowledgements

Not applicable.

Authors' contributions

AS: Results & statistics, manuscript writing and editing, correlated the study concept and design. NK: Idea of the research, correlated the study concept and design, writing the manuscript. SA: Idea of the research, collecting cases. YA: Revising manuscript. All authors read and approved the final manuscript.

Funding

No Funds, sponsorship or financial support to be disclosed.

Availability of data and materials

The datasets used and/or analyzed during the current study are available from the corresponding author on reasonable request.

Declarations

Ethics approval and consent to participate

This study was approved by the Research Ethics Committee of the Faculty of Medicine at Ain shams University in Egypt (FWA 000017585); Reference Number of approval: 216/2019. A written informed consent to participate in this research was given by patients' legal guardian.

Consent for publication

All patients' legal guardian included in this research gave written informed consent to publish the data contained within this study.

Competing interests

The authors declare that they have no competing interest.

Received: 15 March 2021 Accepted: 28 July 2021

Published online: 03 August 2021

References

1. Robinson R, Bhuta S (2011) Susceptibility-weighted imaging: a major addition to the neuroimaging toolbox. *J Neuroimaging* 21(4):309–309. <https://doi.org/10.1111/j.1552-6569.2010.00524.x>

2. Haacke EM, Mittal S, Wu Z et al (2009) Susceptibility-weighted imaging: technical aspects and clinical applications, part 1. *AJNR* 30:19–30
3. Tong KA, Ashwal S, Obenaus A et al (2008) Susceptibility-weighted MR imaging: a review of clinical applications in children. *AJNR Am J Neuroradiol* 29:9–17
4. Duyn J (2013) MR susceptibility imaging. *J Magn Reson* 229:198–207
5. Chalian M, Tekes A, Meodod A et al (2011) Susceptibility-weighted imaging (SWI): a potential non-invasive imaging tool for characterizing ischemic brain injury? *J Neuroradiol* 38(3):187–190
6. Gasparian GG, Sanossian N, Shiroishi MS et al (2014) Imaging of occlusive thrombi in acute ischemic stroke. *Int J Stroke* 10(3):298–305. <https://doi.org/10.1111/ijis.12435>
7. Bosemani T, Poretti A, Orman G et al (2013) Pediatric cerebral stroke: susceptibility-weighted imaging may predict post-ischemic malignant edema. *Neuroradiol J* 26(5):579–583
8. Colbert CA, Holshouser BA, Aaen GS et al (2010) Value of cerebral microhemorrhages detected with susceptibility-weighted MR imaging for prediction of long-term outcome in children with non-accidental trauma. *Radiology* 256:898–905
9. Mittal S, Wu Z, Neelavalli J et al (2009) Susceptibility weighted imaging: technical aspects and clinical applications, part 2. *AJNR Am J Neuroradiol* 30:232–252
10. Wu X, Wu W, Pan W et al (2015) Acute Necrotizing Encephalopathy: an underrecognized clinicoradiologic disorder. *Mediators Inflamm.* <https://doi.org/10.1155/2015/792578>
11. Poyiadji N, Shahin G, Noujaim D et al (2020) COVID-19-associated acute necrotizing encephalopathy: imaging features. *Radiology* 296:E119–120
12. Sahin N, Solak A, Alkilic L (2015) The contribution of susceptibility-weighted imaging (SWI) in occult cerebral vascular malformations in pediatric patients. *Clin Med Rev Case Rep* 2:32. <https://doi.org/10.23937/2378-3656/1410032>
13. Bosemani T, Poretti A, Huisman TA (2014) Susceptibility-weighted imaging in pediatric neuroimaging. *J Magn Reson Imaging* 40(3):530–544. <https://doi.org/10.1002/jmri.24410>
14. Beauchamp MH, Beare R, Ditchfield M et al (2013) Susceptibility weighted imaging and its relationship to outcome after pediatric brain injury. *Cortex* 49(2):591–598
15. Sorimachi T, Morita K, Sasaki O et al (2011) Change in cortical vein appearance on susceptibility-weighted MR imaging before and after carotid artery stenting. *Neurol Res* 33(3):314–318
16. Horie N, Morikawa M, Nozaki A et al (2011) “Brush Sign” on susceptibility-weighted MR imaging indicates the severity of moyamoya disease. *AJNR Am J Neuroradiol* 32(9):1697–1702
17. Mittal P, Kalia V, Dua S (2010) Pictorial essay: susceptibility-weighted imaging in cerebral ischemia. *Indian J Radiol Imaging* 20(4):250–253
18. Thomas B, Somasundaram S, Thamburaj K et al (2008) Clinical applications of susceptibility weighted MR imaging of the brain- a pictorial review. *Neuroradiology* 50(2):105–116
19. Sinha V, Purohit D, Karthikeyan Y (2017) Role of magnetic resonance imaging in unconscious patients due to diffuse axonal injury and its prognostic value. *Ind J Neurotrauma* 32(7):312–344
20. Sultan A, Elshafey K, Hassaniien O et al (2020) Magnetic resonance susceptibility weighted in evaluation of cerebrovascular diseases. *Egypt J Radiol Nucl Med.* <https://doi.org/10.1186/s43055-020-00198-y>
21. Hamdeh A, Marklund N, Lannsjö M et al (2017) Extended anatomical grading in diffuse axonal injury using MRI: hemorrhagic lesions in the substantia nigra and mesencephalic tegmentum indicate poor long term outcome. *J Neurotrauma* 66(3):37–45
22. Babikian T, Merkley T, Ronald C (2015) Chronic aspects of traumatic brain injury: review of Literature. *J Neurotrauma* 147(12):235–277
23. Ashwal S, Babikian T, Gardner Nichols J et al (2006) Susceptibility-weighted imaging and proton magnetic resonance spectroscopy in assessment of outcome after pediatric traumatic brain injury. *Arch Phys Med Rehabil* 87(12):S50–58
24. Lawrence T, Pretorius M, Ezra M et al (2017) Early detection of cerebral Microbleeds following traumatic brain injury using MRI in the hyper-acute phase. *Neurosci Lett* 655(7):143–150
25. Seo HE, Hwang SK, Choe BH et al (2010) Clinical spectrum and prognostic factors of acute necrotizing encephalopathy in children. *J Korean Med Sci* 25(3):449–453
26. Ormitti F, Ventura E, Summa A et al (2010) Acute necrotizing encephalopathy in a child during the 2009 influenza A(H1N1) pandemic: MR imaging in diagnosis and follow-up. *Am J Neuroradiol* 31(3):396–400
27. Manara R, Franzoi M, Cogo P et al (2006) Acute necrotizing encephalopathy: combined therapy and favorable outcome in a new case. *Childs Nerv Syst* 22(10):1231–1236
28. Sparcia G, Speciale C, Banco A et al (2016) Accuracy of SWI sequence compared to T2* weighted gradient echo sequences in the detection of cerebral cavernous malformations in the familial form. *J Neuroradiol* 29(5):325–336
29. El-Serougy LG, El-Rakhawy MM, Ashamalla GA et al (2017) Reliability of magnetic susceptibility weighted imaging in detection of cerebral microbleeds in stroke patients. *Egypt J Radiol Nucl Med* 48(1):225–229
30. Bosemani T, Verschuuren SI, Poretti A et al (2013) Pitfalls in susceptibility-weighted imaging of the pediatric brain. *J Neuroimaging* 24(3):221–225

Publisher's Note

Springer Nature remains neutral with regard to jurisdictional claims in published maps and institutional affiliations.

Submit your manuscript to a SpringerOpen® journal and benefit from:

- Convenient online submission
- Rigorous peer review
- Open access: articles freely available online
- High visibility within the field
- Retaining the copyright to your article

Submit your next manuscript at ► [springeropen.com](https://www.springeropen.com)